ingegneria sismica
International Journal of Earthquake Engineering
Anno XLIII - Num. 2 - 2026

Research on the operation mode and optimized scheduling strategy of new energy hydrogen production

Shilong Liu[1,*] *and Chengbang Ma*[1]

[1] Qinghai Huanghe Hydropower Development Co., Ltd., Xining, Qinghai, 810000, China

SUMMARY: *In order to improve the smoothness of wind power consumption and grid-connected power, for the single investment in new energy hydrogen production mode faces the dilemma of low equipment utilization and operating losses. In this research paper, we have devised a novel operation model for a multi-principal united enterprise. This model depends on the classical Shapley value method to deal with the calculation of operation costs, the allocation of investment costs, and the distribution of benefits. On this basis, an optimal scheduling model of new energy hydrogen production system based on the objective function of economy and power supply reliability is proposed, and the model is solved by the improved slime mold algorithm, which improves the searching efficiency by initializing the population with Sobol's low-discrepancy sequences, and introduces the searching strategy obeying the Levy distribution to enhance the optimization ability of the algorithm. Simulation analysis results show that the proposed strategy can effectively utilize the time-sharing tariff mechanism and obtain significant economic benefits while maximizing the utilization of wind and light. By sharing the capacity of multiple subjects, the overall economy of the hydrogen production plant is greatly improved, and a win-win cooperation among multiple parties is realized. The research results of this study provide a new angle for the building and running management of large-scale new energy use facilities that have whole-network public-benefit attributes.*

KEYWORDS: *New energy hydrogen production; multi-principal operation; Shapley value method; improved slime mold algorithm; scheduling optimization*

1 Introduction

Energy is the basis for supporting the development of national economy and promoting social progress, and the development of economy and society can never be separated from the support of energy. In order to cope with the global warming problem, the development of cleaner, sustainable, safe and efficient modern energy has become a consensus reached by countries around the world [1]. Compared with traditional thermal power generation, new energy generation has many advantages, such as environmentally friendly and inexhaustible resources. Therefore, it will become an important support to promote the transformation of the power system to clean and low-carbon. Under the fast development of new-energy electricity production, which is represented by wind and photovoltaic energy, the problem of abandoning wind and solar power has become more and more obvious. This problem is originated from the cannot-predict property of wind and solar power generation and their against-peak characteristics, which therefore have hindered the use of new energy[2-4]. In order to better utilize new energy, many countries have issued a number of policy documents to promote new

*goajjian665@yeah.net
https://doi.org/10.65102/is2026578
Published: 30 April, 2026

energy-rich areas to build electricity to hydrogen, electricity to methane and other large-scale consumption equipment, the abandoned wind, abandoned light into fuel gas storage or utilization, so as to effectively broaden the new energy consumption channels [5-7].

The combination of wind energy, photovoltaic power and other kinds of new energy power generation together with water electrolysis for hydrogen manufacture provides many advantages. First of all, it can utilize the rapid power-regulation abilities of water-electrolysis hydrogen-generation equipment. This can assist in alleviating the unstable situation which a high percentage of new energy sources can bring to the electric power network. Secondly, it makes possible the effective use of low-cost wind and solar energy which, if not used, would become waste. Through this kind of operation, it has effectively reduced the cost of water electrolysis which is used for the producing of hydrogen [8-11]. Hydrogen produced from new energy power has become a sustainable green energy, which has attracted extensive attention worldwide. Notwithstanding the great progressions in the technique of manufacturing hydrogen via new energy origins, its large-scale application is still challenging in the current market environment due to cost constraints [12]. Therefore, exploring a new business model to overcome the cost constraints will help improve the comprehensive competitiveness of new energy hydrogen production, thus laying a solid foundation for the large-scale popularization and development of new energy hydrogen production. In this context, the operation mode and optimized scheduling of new energy hydrogen production deserve further study.

New energy electrolytic water hydrogen production system can be categorized into on-grid and off-grid states according to the connection with the grid to meet different application requirements. Off-grid hydrogen production is often applied to island grids or microgrids containing new energy with weak autonomy, while grid-connected wind-coupled hydrogen production has greater flexibility and is important for promoting new energy consumption and reducing carbon emissions from hydrogen production [13, 14]. Fan and his work companions have brought forward three power handling strategies for the energy handling of a separated electric network that includes wind power for the making of hydrogen. The research results showed that the extra electric energy of renewable energy sources under the off-grid condition and the electricity storage condition of the storage battery control the operation methods of water electrolysis for making hydrogen and fuel cells [15]. Wei et al [16] investigated the power-efficiency characteristics of electrolytic water for hydrogen production, and proposed an optimal scheduling strategy for power systems that takes into account the efficiency of hydrogen production and the consumption of wind power. The strategy was proposed by Wei et al.

Electrolyzed water to hydrogen production equipment is expensive and has a limited service life, and its depreciation cost is also considerable.In a extremely competitive market, if one does not have a reasonable working method, throwing capital into the construction of facilities for making hydrogen by electrolyzing water will bring about great losses.Niu and [17] his work team have conducted examination on the changes of the efficiency in dynamic hydrogen generation. They utilized the Non-dominated Sorting Genetic Algorithm II and entropy methods to carry out optimization on the working of the hydrogen electrolysis device in a wind-battery energy storage-alkaline electrolyzer system. The goal of this optimization work was to promote the working effect of the system.

Farag and [18] his working group designed an overall formula for the perfect running and management of dispersed and concentrated electrolytic hydrogen production and storage systems. The goal was to promote the system's net profit through making use of the sale of the produced hydrogen and its grid-supporting service behaviors. Guo et al [19] designed an operationally optimal configuration and production model in a renewable energy hydrogen production system with downstream constraints, which obtained the lowest full life cycle cost

of hydrogen in a PV/wind grid-connected scenario and achieved a much lower number of start/stop cycles than typically required.Liu [20] used the hydrogen producing technology which is based on water electrolysis and hydrogen fuel cells to carry out optimal arrangement in an integrated electricity-heat-hydrogen energy system under many kinds of operation modes. This method reduces every day working costs and corrects data prediction errors, hence therefore promoting the stability of the system's running. Sun and [21]his work group have completed an optimization work for the structure and operation scheme of a hydrogen refueling station which is equipped with on-site electrolysis to produce hydrogen. They achieved this work through the simulation of the refueling behaviors of the station and the formulation of a hydrogen demand prediction model. Therefore, the average time of breaking even has been cut down by 3.3 years. Furthermore, they have obtained the minimization of both the installation investment and the total cost.Wu et al [22] transformed the wind-photo-hydrogen cooperative operation and revenue distribution under the market mechanism into the process of seeking Nash negotiation solution, which solved the problem of revenue distribution after the wind-hydrogen combination, and was superior to the method based on the coalition game model.

Large-scale hydrogen production units are usually invested in construction and operation by a single subject, and the pressure of depreciation cost is concentrated, resulting in poor overall project economics. This paper proposes a new equity model of multi-principal joint venture hydrogen plant, which shares the production capacity of hydrogen plant among multiple participants by integrating the investment costs of wind power, photovoltaic, and other multi-source investment entities, sharing the investment costs and depreciation costs, and reducing the operation pressure of multiple entities. After that, a comprehensive construction of the day-ahead optimal arrangement model is carried out. For the sake of promoting the optimization ability of the slime mold algorithm, the Sobol low-discrepancy sequence initialization method and the Levy flight method are introduced into it by us. The strengthened slime mold algorithm is hence utilized to settle the day-ahead optimal arrangement model. In the end, according to the forecast data of wind and photovoltaic electricity production, the reasonability and cost efficiency of both this model and the scheduling optimization model have been checked and confirmed.

2 Operational models for new energy hydrogen production

2.1 Barriers faced by single investors

Hydrogen plants are expensive to invest in and have limited capacity. It will be difficult for the plant to operate at a loss by only consuming abandoned wind, and to be profitable it must consume other components of electricity to increase the plant's utilization rate.

Both the network side and the new energy side of the single investor is difficult to achieve profitability, mainly because of the existence of price barriers make the device can not be in a single subject to enjoy the price advantage of both sides. It is not difficult to imagine that if the production capacity of the hydrogen production equipment is shared, combining the advantages of both sides, and realizing the sharing of depreciation costs: consuming wind abandonment at zero cost during the time when there is wind abandonment, and purchasing electricity at the internal price of the plant and grid side during the time when there is no wind abandonment in order to improve the utilization rate of the hydrogen production equipment, then it can obtain a much better economy, and its chances of making a profit will be greatly increased.

2.2 New Energy Hydrogen Production Operation Model Based on Multiple Subjects

We start from the concept of the cooperative economy, the sharing of hydrogen production equipment can be effectively achieved through multi-agent joint venture construction/operation or third-party construction and time-share leasing to overcome the "friction" brought by the barriers of transaction costs. Figure 1 shows the multi-agency joint venture construction/ operation model, which will be discussed in the following:

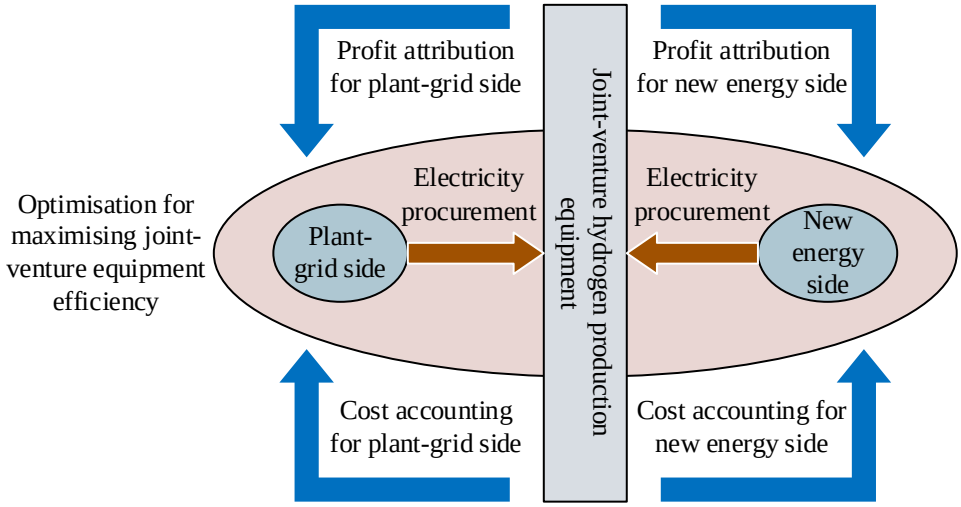

Figure 1: Multi-subject joint venture system of hydrogen production

1) The new energy side and the plant network side are the parent company, and the economic entity operating the hydrogen production unit is the subsidiary. The subsidiaries shall separately account for the related transactions with the parent company and pay for the newly increased daily operating costs of the parent company as a result of the business practices of investing in and operating the subsidiaries;

2) Carry out optimization works for the purpose of maximizing the benefits obtained from the cooperative hydrogen production factory;

3) Construction costs and net profits incurred as a result of the investment and business practices of the hydrogen production facility shall be shared and shared by both parties in accordance with the Shapley value method to realize the contribution ratio.

2.2.1 Daily operating cost accounting for the new model

Daily operating costs are categorized into floating and fixed costs. Floating costs are the reduced revenues of the wind farm due to the use of electricity from the wind farm and the increased costs on the plant side due to the purchase of electricity from the plant grid side, while fixed costs are the depreciation of the equipment, excluding for the time being other costs such as personnel expenses.

The principle of variable cost compensation is to pay for any new increase in joint venture-side costs or decrease in joint venture-side revenues due to power purchases by any factor company, i.e:

$$C_i\left(P_0,\Delta P_i\right)=M_i\left(P_0\right)-M_i\left(P_0,\Delta P_i\right)+F_i\left(P_0,\Delta P_i\right)-F_i\left(P_0\right) \tag{1}$$

where: P_0 is the total generating power of the original i th joint venture; ΔP_i is the newly

increased power due to the power purchase of its factor company; M_i and F_i are the total revenue and total cost corresponding to the power.

Specifically for the objects in the paper, at moment t, the purchase of power by the hydrogen production equipment reduces the wind farm's sales revenue C_1^t by:

$$C_1^t = \left(P_{0-Wind}^t - P_{Wind}^t \right) p_{online} \tag{2}$$

For the grid side, it is necessary to account for the increased cost of coal consumption on the grid side due to the purchase of electricity by the hydrogen production equipment, but it must also be considered that the purchase of electricity from wind farms by the hydrogen production equipment may also reduce the expenditure on the grid side for the acceptance of wind power, and therefore the increased cost C_2^t on the grid side is the increase in the cost of coal consumption less the lesser amount spent on acquiring on-grid wind power, denoted as follows:

$$\begin{aligned} C_2^t = & \sum_{i=1}^{n} p_1 \left[a_i \left(P_i^t \right)^2 + b_i P_i^t + c_i \right] \\ & - \sum_{i=1}^{n} p_1 \left[a_i \left(P_{0\sim i}^t \right)^2 + b_i P_{0\sim i}^t + c_i \right] - \left(P_{0\text{-}Wind}^t - P_{Wind}^t \right) p_{online} \end{aligned} \tag{3}$$

where: n is the number of thermal power units, a_i, b_i, c_i is the fuel cost coefficient of the i th unit; p_1 is the price of fuel; $P_{0\sim i}^t$, P_i^t is the power output of the conventional generating unit i in the t th time before and after the purchase of electricity by hydrogen production equipment.

When we make the addition of the values from Equations (2) and (3), it is thus clearly seen that the total cost of the hydrogen production plant is fundamentally equal to the increased cost of coal usage. Nevertheless, this expense is distributed among the two bodies in accordance with the provisions given in Equations (2) and (3).

The depreciation cost of hydrogen production equipment is a fixed cost, which will not affect the optimization result of the scheme, but because the investment amount of the related parties based on the Shapley value method is not the same, so it is necessary to pay the parties in proportion to the investment amount to avoid the friction caused by the understanding of the difference in the investment amount.

The daily depreciation C_d using the annual average method is:

$$C_d = \frac{C_I - C_R}{365Y} \tag{4}$$

where: C_I is the original value of the hydrogen production equipment; C_R is the salvage value, which is taken as $30\%C_I$; and Y is the estimated service life.

2.2.2 Investment cost sharing and profit sharing in the new model

Reasonable sharing of costs and fair distribution of profits are the prerequisites for multiple subjects to reach cooperation. The classical Shapley value method is able to proportionally distribute the due benefits according to the participation and contribution of members, which

can ensure the results are fair and reasonable. At the same time, it objectively realizes the economic consistency of each participating subject, fully mobilizes the enthusiasm of the participants, helps to reinforce the alliance, and ensures an orderly market. On the opposite side, in the common multi-agent method, there exists no unified entity that sits above separate agents to coordinate the benefits of all participating sides. From objective perspective, the economic benefits of market participants are in a condition of mutual conflict. The formulation of each side's own strategies and the promotion of self-optimization are carried out under the framework of a non-cooperative game in the process of competition. This circumstance may bring about the "prisoner's dilemma," hence it can greatly influence the whole economic situation. In this research work, the Shapley value method is utilized by us to inspect the economic benefits of the competing participating sides.In this present research paper, the method of Shapley value is utilized to study the income allocation of joint operation enterprises. In the theory aspect, this method can reach the goal of a result that benefits all sides together.

When n members engage in an economically profitable activity, each member makes a profit, but when n members form a coalition, the total profit of the coalition is greater than the sum of the profits made by the n members individually from the economic activity.

Let the set $N=\{1,2,\cdots,n\}$ be satisfied if for any subset S of N (any one of the n persons cooperating) corresponds to a real-valued function $V(S)$:

$$\begin{cases} V(\phi)=0 \\ V(S_1 \cup S_2) \geq V(S_1)+V(S_2), \quad S_1 \cap S_2=\phi \end{cases} \tag{5}$$

Then we call $[N,V]$ the cooperative response of n people and V the characteristic function of the response, where $V(S)$ is the gain of cooperation S.

If we remember $\Phi=(\Phi_1(v),\Phi_2(v),\cdots,\Phi_n(v))$ as the allocation vector of the cooperative coalition, where $\Phi_i(v)$ denotes the allocation due to the ith member's investment equity and profit in the cooperative game $[N,V]$, i.e., the Shapley value, which is computed by the formula

$$\Phi_i(v)=\sum_{i \subset S} w(|S|)\left(v(S)-v(S \setminus i)\right), \quad i=1,2,\cdots,n \tag{6}$$

where: $w(|S|)=(n-|S|)!(|S|-1)!/n!$; $|S|$ denotes the number of members in the coalition; n is the number of members in the bureau; and $v(S \setminus i)$ denotes the contribution of the member i to the coalition S.

In this paper, the wind farm, plant and grid side joint venture operation of hydrogen production equipment distributes the revenue, which is suitable for the application conditions of Shapley value method. Wind farms, plant and network side investment alone and the two joint venture operation of hydrogen production equipment constitute a cooperative alliance space $S=(\{W\},\{F\},\{W,F\})$, and the revenue vector of the three combinations can be expressed as $V=(V(\{W\}),V(\{F\}),V(\{W,F\}))$. The allocation vector $\Phi=(\Phi_1(v),\Phi_2(v))$ of the cooperative coalition is strictly enforced in the specific benefit allocation. It can be seen that the principle of "distribution according to work" of the classical Shapley value method theoretically realizes the fairness and reasonableness of the distribution results, and objectively

proves the practical feasibility of the new energy-side and plant-network-side joint ventures of hydrogen production equipment.

2.3 The whole-subject relationship in the new paradigm

The implementation of any scheduling strategy is a two/multiparty game, which is briefly analyzed to demonstrate the feasibility of the strategy.

For the i th subject, its final payoff $S_{i\text{-}total}$ is:

$$S_{i\text{-}total}\left(P_0,\Delta P\right)=M_i\left(P_0\right)-F_i\left(P_0,\Delta P\right)+C_i\left(P_0,\Delta P\right)+\Phi_i \tag{7}$$

Substituting into equation (1), there is:

$$S_{i\text{-}total}\left(P_0,\Delta P\right)=M_i\left(P_0\right)-F_i\left(P_0\right)+\Phi_i \tag{8}$$

And Φ_i is the cooperative allocation of revenue, it can be seen that the interests of wind farms, plant and network side of the subject and the interests of the two joint venture hydrogen production device is highly consistent, hydrogen production equipment to maximize the interests of the same time, but also in line with the principle of maximizing the interests of each participant in the main body, the results of this is the Pareto optimal in the cooperative game, which can be acceptable for the parties involved in the joint venture. This result is the Pareto optimal in the cooperative game, which can be accepted by all parties of the joint venture. It can be seen that the optimization of the scheduling strategy with the maximization of the interests of the hydrogen plant will have realistic feasibility.

3 Optimized scheduling model for new energy hydrogen production system and its solution

3.1 Optimization model of new energy hydrogen production system

3.1.1 Objective function

The optimization model is constructed by selecting two objectives: economy and power supply reliability. The first objective function is to minimize the comprehensive operation and maintenance cost f_1 of the system in one day, which contains the operation and maintenance expenditure of the wind turbine, lithium iron phosphate battery, and two kinds of electrolysis baths, together with the income which is produced by hydrogen sales.

$$f_1=\min\left(C_d-C_{H_2}\right) \tag{9}$$

$$C_d=\sum_{t=1}^{T}\sum_{i\in\phi}K_iN_iP_i(t) \tag{10}$$

$$C_{H_2}=\sum_{t=2}^{T}C_1Q_{H_2}(t) \tag{11}$$

where: C_d is the daily operation and maintenance cost of the system; C_{H_2} is the revenue from the sale of hydrogen; and ϕ is the set of all units of the system; K_i is the unit O&M cost of each unit of the system; N_i is the number of units of the system; $P_i(t)$ is the output power of each unit at moment t; C_1 is the hydrogen price; $Q_{H_2}(t)$ is the volume of hydrogen sold at moment t.

This paper is set in the context of a stand-alone isolated microgrid, so the reliability of the system operation needs to be assessed. Under the premise of meeting the load demand, wind power and photovoltaic power are absorbed as much as possible to ensure a small power deficit and minimize the surplus of wind and light, so the second objective function is chosen to minimize the absolute value of the difference between the system output and the load, f_2:

$$f_2 = \min\left(\sum_{t=1}^{T}\left|P_{e\&g}(t) - P_{e\&c}(t)\right|\right) \tag{12}$$

$$P_{e\&g}(t) = P_{WT}(t) + P_{PV}(t) - P_{SB}(t) \tag{13}$$

$$P_{e\&c}(t) = P_{load}(t) + P_{ele}(t) + P_{cell}(t) \tag{14}$$

where: $P_{e\&g}(t)$ is the output capability of the electric power production system and the energy storage system at the t moment; $P_{e\&c}(t)$ is the absorbed power of the power consumption system at the t moment; and $P_{load}(t)$ is the load demand at the t moment.

Transforming f_2 into a reliability cost model, the power shortage penalty cost $C_{In\&p}$ and the power surplus penalty cost $C_{sur\&p}$ are introduced:

$$f_2' = \min\left(\sum_{t=1}^{T}\left|P_{e\&g}(t) - P_{e\&c}(t)\right|C(t)\right) \tag{15}$$

$$C(t) = \begin{cases} C_{sur\&p} & P_{e\&g}(t) - P_{e\&c}(t) > 0 \\ C_{In\&p} & P_{e\&g}(t) - P_{e\&c}(t) \le 0 \end{cases} \tag{16}$$

$$C_{In\&p} = BC_{ave} \tag{17}$$

where: $C(t)$ is the penalty cost at moment t; B is the shortage penalty coefficient; and C_{ave} is the average electricity price.

The ameliorated credibility model has incorporated economic measuring norms, hence the multi-goal function is transformed by people into the one-goal function.

$$Z = f_1 + f_2' \tag{18}$$

where Z is the total system cost, which consists of the daily operation and maintenance cost and the reliability cost.

3.1.2 Constraints

1) Power balance constraints.

$$P_{WT}(t)+P_{PV}(t)=P_{load}(t)+P_{ele}(t)+P_{cell}(t)+P_{SB}(t) \tag{19}$$

2) Micro-source output constraints.

$$P_{WT,\min}\le P_{WT}(t)\le P_{WT,\max} \tag{20}$$

$$P_{PV,\min}\le P_{PV}(t)\le P_{PV,\max} \tag{21}$$

where: $P_{WT,\max}$, $P_{WT,\min}$ are the upper and lower limits of wind turbine output; $P_{PV,\max}$, $P_{PV,\min}$ are the upper and lower limits of PV cell output.

3) Energy storage device constraints.

$$P_{SB,\min}\le P_{SB}\le P_{SB,\max} \tag{22}$$

$$S_{OC\min}\le S_{OC}\le S_{OC\max} \tag{23}$$

$$C_{soc}(0)=C_{soc}(T) \tag{24}$$

where: $P_{SB,\max}$, $P_{SB,\min}$ are the maximal and minimal border ranges of the power mutual action inside the energy storage device; $S_{OC\max}$, $S_{OC\min}$ are the maximal and minimal limit lines of the electric charge degree inside the energy storage device; and Eq. (23) is the restriction on the circle working of the storage equipment is arranged to ensure its ability to finish circle jobs.

4) Electrolyzer power constraints.

$$\eta_{ele,\min}\le\eta_{ele}\le\eta_{ele,\max} \tag{25}$$

$$\eta_{cell,\min}\le\eta_{cell}\le\eta_{cell,\max} \tag{26}$$

$$\left|P_{ele}(t+1)-P_{ele}(t)\right|\le\Delta P_{ele,\max} \tag{27}$$

$$\left|P_{cell}(t+1)-P_{cell}(t)\right|\le\Delta P_{cell,\max} \tag{28}$$

where: $\eta_{ele,\max}$, $\eta_{ele,\min}$ are the maximum and minimum numerical values of the efficiency of the Proton Exchange Membrane (PEM) electrolyzer device; $\eta_{cell,\max}$, $\eta_{cell,\min}$ are the upper and lower limits of alkaline electrolyzer efficiency; $\Delta P_{ele,\max}$, $\Delta P_{cell,\max}$ are the maximum rate of climb of the electrolyzer.

5) Electrolyzer start-stop constraint.

$$\begin{cases} \sum_{m=0}^{T_{on}-1} u(t+m) \geq T_{on}[u(t)-u(t-1)] \\ \sum_{m=0}^{T_{off}-1} [1-u(t+m)] \geq T_{off}[u(t-1)-u(t)] \\ 0 \leq S_{on} \leq S_{on,\max} \\ 0 \leq S_{off} \leq S_{off,\max} \end{cases} \tag{29}$$

where: T_{on}, T_{off} is the minimum start/stop time of PEM electrolyzer; $u(t)$ is the start/stop state of PEM electrolyzer at the moment of t, which takes the value of 0 or 1 (0 means shutdown, 1 means startup); S_{on} is the number of startup times per day; $S_{on,\max}$ is the maximum number of daily startups; S_{off} is the number of daily shutdowns; $S_{off,\max}$ is the maximum number of daily shutdowns. Considering the start-stop characteristics of alkaline electrolyzer, it is set to be normally open; at the same time, in order to avoid intermittent operation of PEM electrolyzer, it is set to have start-stop constraints.

3.1.3 Operational control strategies

The operation control strategy of the system affects the power distribution, which directly affects the operation efficiency of the system. When the system is working, the fan, photovoltaic output and energy storage device discharge sometimes can not meet the load and two electrolyzer are working in the optimal interval, in order to ensure the economy and reliability of the system operation as much as possible, set up two working states, so that the system in different situations to choose different operation control strategy. The alkaline electrolyzer is inconvenient to start and stop, so it is set to be normally open; while the PEM electrolyzer is more flexible in comparison, so it is set to the following control strategy.

Working state 1: When the output of wind turbine and photovoltaic cannot meet the load demand, i.e., $P_{WT}(t)+P_{PV}(t) \leq P_{load}(t)$, PEM electrolyzer is shut down, the alkaline electrolyzer operates in the optimal operation interval for continuous hydrogen production, and the energy storage device is discharged.

Operating state 2: When the output of wind turbine and photovoltaic is greater than the load demand, i.e., $P_{WT}(t)+P_{PV}(t) > P_{load}(t)$, the alkaline electrolyzer operates in the optimal operation interval, and the PEM electrolyzer is utilized to absorb the residual power. If $P_{WT}(t)+P_{PV}(t) > P_{load}(t)+P_{ele}(t)+P_{cell}(t)$, the energy storage device is charged; if $P_{WT}(t)+P_{PV}(t) < P_{load}(t)+P_{ele}(t)+P_{cell}(t)$, the energy storage device discharges.

3.2 Optimization model solution method for new energy hydrogen production system

The process of solving a scheduling model, which can also be called an optimization process, is the process of finding the optimal solution among all feasible solutions to a given problem. Optimization problems are one of the most important and popular research topics today and can be found in the core processes of various tasks, such as medicine, economics and energy. Optimization problems can be solved in a variety of ways, but they can be broadly classified into two types, namely traditional optimization algorithms and intelligent optimization algorithms. Traditional optimization algorithms for solving this problem are usually based on gradient-based iterative methods such as conjugate gradient method, Newton's method, and so on.

This method can only be used for strictly convex function problems because of the need for gradient information. Group intelligence algorithms, as one of the intelligent algorithms, are inspired by the behavior of biological populations in nature, also known as meta-heuristic algorithms, which are often used to simulate the mutual communication and cooperation among individuals of different biological populations by using mathematical modeling to establish different kinds of group intelligence algorithms, such as particle swarm algorithm, ant colony algorithm and firefly algorithm Although the specific problems of microgrid scheduling are different, and the used Although the specific problems of microgrid scheduling are different and the intelligent algorithms used are also different, when using intelligent algorithms to solve the problem of optimal scheduling of new energy hydrogen production system, it is generally necessary to go through the following processes:

1) Consider and screen out the appropriate type of power generation equipment in the new energy hydrogen system.

2) Construct a mathematical model of the problem to obtain the objective function to be studied.

3) Construct the constraints that need to be considered to solve the problem.

4) Carry out the search for the solution that has the best fitting degree for the ideal scheduling model of the new-energy hydrogen production system.

The slime mold algorithm is a meta-heuristic algorithm that simulates the morphological and behavioral changes in the foraging process of slime molds. The algorithm has a simple structure, few adjustment parameters, high scalability, and excellent performance in function optimization and design problems of engineering, and has been successfully applied to different engineering fields such as motor control parameter optimization, bioengineering, path planning and image segmentation performance optimization.

3.2.1 Design of Improved Mucilage Algorithm

The main mathematical model for simulating slime mold foraging can be expressed as:

$$X(it+1)=\begin{cases} LB+(UB-LB)r, r<z \\ X_b(it)+v_b\left(X_A(it)-X_B(it)\right), r<p \\ v_c X(it), r\geq p \end{cases} \tag{30}$$

where UB and LB are the upper and lower boundaries of the optimality-seeking region, respectively, r denotes a random number between $[0,1]$, $z=0.03$ is a customization parameter, X_s is the position of ideal slime mold sample in this current iteration, W is the fitness weights, X_A and X_B are the two randomly selected individual positions, $v_3\in[-a,a]$ is the range parameter, v_2 decreases linearly from 1 to 0, $X(it)$ is the current iteration position, $X(it+1)$ is the position after updating the iteration, it is the number of current iterations, and the parameters a and p are respectively:

$$a=\arctan h\left(1-\frac{it}{it_{\max}}\right) \tag{31}$$

$$p=\tanh\left|S(i)-DF\right| \tag{32}$$

where $it_{\max}$ is the maximum number of repeat times, $S(i)$ is the presently individual's body ability score, and DF is the best fitness value among all previous iterations.

The adaptation weight W can be expressed as:

$$W\left(Sf(i)\right)=\begin{cases}1+r_1\log\left(\dfrac{BF-S(i)}{BF-WF}+1\right), i=ib\\ 1-r_1\log\left(\dfrac{BF-S(i)}{BF-WF}+1\right), i=ia\end{cases} \tag{33}$$

$$SI(i)=sort\left(S(i)\right) \tag{34}$$

where BF denotes the best fitness value of the current iteration, WF denotes the worst fitness value of the current iteration, $i=ib$ denotes the slime mold individual with the top half of the population fitness value, $i=ia$ denotes the other slime mold individuals, and $SI(i)$ is the result after the fitness value is sorted.

However, because the optimization mechanism of the traditional slime mold algorithm is relatively simple, while the scheduling model in this paper needs to simultaneously consider the different states and different constraints of multiple units in the system, which is a multiconstraint, multivariate and high-dimensional nonlinear problem,when we use the algorithm to deal with problems, it has the shortcomings that it is easy to have premature convergence and be caught in local optima. Therefore, this paper makes the following improvements to the algorithm and solves the scheduling model using the improved slime mold algorithm.

(1) Sobol sequence initialization improved slime mold algorithm

The initial placing of the population will produce a special influence on the early stage of the algorithm's search efficiency and accuracy, especially when dealing with high-dimensional problems, the initial value of the population if the initial value of the population as far as possible uniformly distributed in the search domain, the initialization of the population obtained can ensure that the population has a good diversity and improve the search efficiency of the algorithm. For this reason, this paper adopts Sobol low-difference sequence initialized population, which is a deterministic proposed random number sequence, with a wide range of sampling and sampling more uniform characteristics. Let the value range of the initial solution be $[x_{\min}, x_{\max}]$, and the proposed random number $\varphi_n \in [0,1]$ generated by the Sobol sequence, then the initial position of the population can be expressed as:

$$x_n = x_{\min} + \varphi_n\left(x_{\max} - x_{\min}\right) \tag{35}$$

(2) Levy Flight Improved Sticky Mushroom Algorithm

Along with the SMA algorithm carries out iteration step by step to look for the optimal result, therefore the global search ability of this algorithm has gradual decrease. This circumstance causes that the SMA algorithm has very big probability to fall into a local optimal point. Lévy flight is a kind of short-step search and long-step search combined with random wandering, this obey Lévy distribution search method makes Lévy flight has a good global search ability. The formula for simulating the step size of the Lévy flight can be expressed as:

$$levy=\frac{\mu}{|v|^{1/\gamma}} \tag{36}$$

where $\gamma = 1.5$ is a constant and μ and v follow a normal distribution, Eq:

$$\mu \sim N\left(0, \sigma_\mu^2\right) \tag{37}$$

$$v \sim N\left(0, \sigma_v^2\right) \tag{38}$$

$$\sigma_\mu = \left\{ \frac{\Gamma(1+\gamma)\sin(\pi\gamma/2)}{\Gamma[(1+\gamma)/2]2^{(\gamma-1)/2}} \right\}^{1/\gamma} \tag{39}$$

$$\sigma_v = 1 \tag{40}$$

The algorithm's improved position update formula is:

$$X(it+1) = \begin{cases} LB + (UB - LB)r, r < z \\ X_b(it) + 0.05\ levy\ \otimes \left(WX_A(it) - X_A(it)\right), r < p \\ v_c X(it), r \geq p \end{cases} \tag{41}$$

3.2.2 Improvement of the general flow of the slime mold algorithm

The flowchart for solving the scheduling model in this chapter using the Improved Sticky Mushroom Algorithm (ISMA) is shown in Fig. 2, in which each Sticky Mushroom individual represents a set of all units at different times of the day, i.e., there exists a one-to-one mapping relationship between the Sticky Mushroom individual and the unit's output schedule.

Step 1 You should input the system parameters and the parameters of the ISMA algorithm. The system parameters include the power of wind and solar renewable energy resources, the power that the load needs, as well as the upper and lower limits and restriction conditions of the unit output. At the same time, the parameters of ISMA algorithm are constituted by the slime mold population size, the variable dimension number, and the maximum iteration count.

Step 2 Make use of the upper limit and lower limit of the unit power. Next, we employ the Sobol sequence for carrying out the mapping of the starting position of the slime mold.

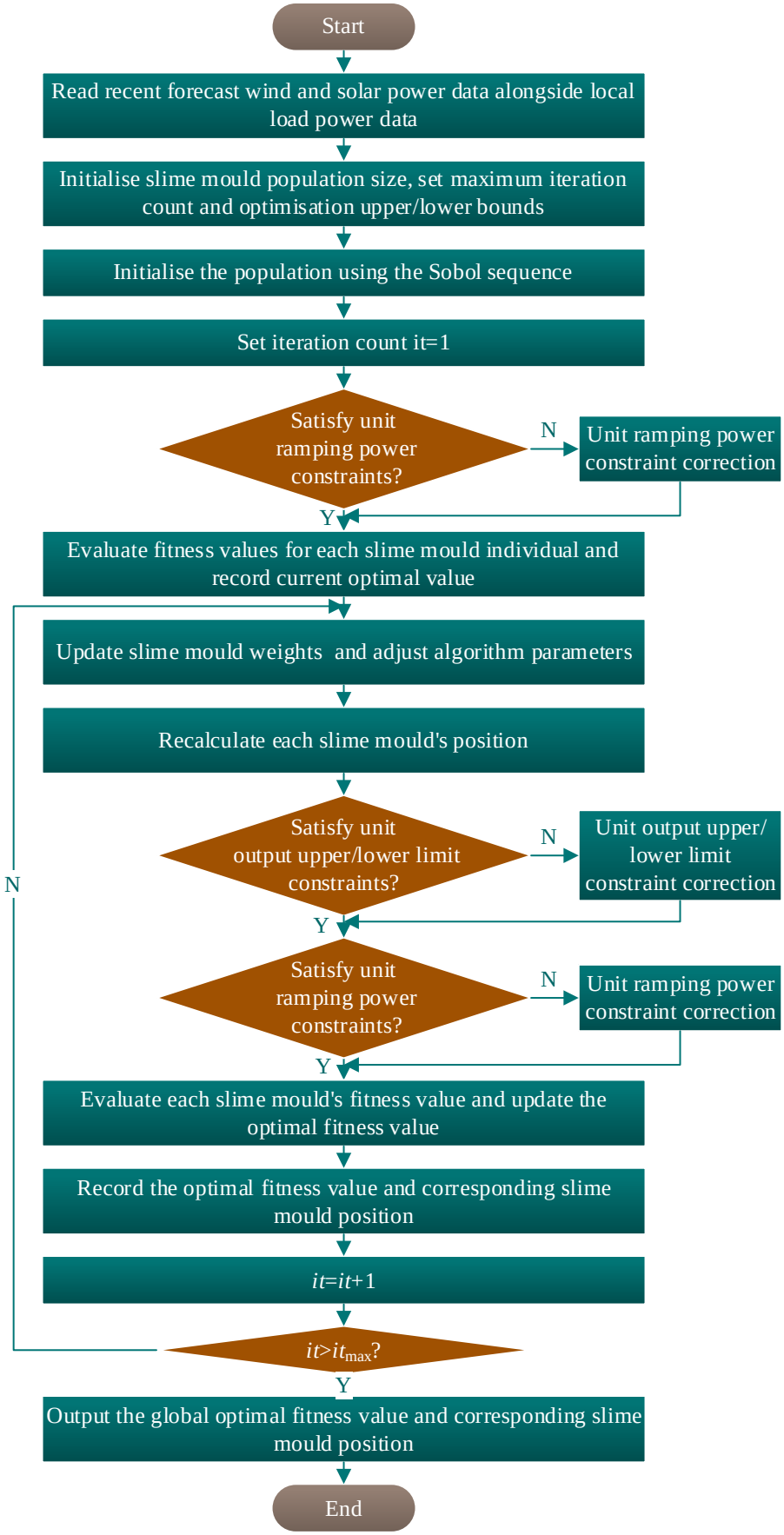

Figure 2: The flow chart of improved SMA

Step 3 At this point, the upper and lower bound constraints of the unit must be satisfied, and only the climbing power constraint mapped by each slime mold individual is corrected.

Step 4 Calculate the scheduling objective function and update the current optimal fitness value and the optimal slime mold location.

Step 5 Recalculate the algorithm parameters such as weights W and update the location of each slime mold individual.

Step 6 Carry out successive adjustments on the upper and lower limit constraint conditions of the unit, and also carry out that on the climbing power constraint condition of each slime mold.

Step 7 Carry out the assessment of the fitness value for every single individual slime mold sample specimen. After that, you shall record the total optimum fitness score together with the position of the individual slime mold which has obtained this score.

Step 8 The current number of iteration times is added by one. In the circumstance that the current iteration number does not exceed the maximum iteration number, you should go forward to Step 5. On the opposite side, if it truly surpasses the maximum iteration number, hence output the optimal scheduling goal value and the system unit power value which correspond to the individual slime mold.

3.3 ISMA algorithm performance testing and analysis

For the purpose of evaluating the optimization effect and steady property of the improved mucilage algorithm, one optimization comparison experiment has been conducted. This test uses the standard test function and a part of the CEC2017 test functions. In the benchmark test function, the single-peak test function has one and only one global optimal solution. This characteristic is helpful for the comprehension of the development capability of the optimization algorithm. In the present research, the Step Function (F1), which is a single-peak testing function, has been employed by us. The multi-peak testing function possesses many local minimum points. This characteristic helps people to comprehend the capability of the optimization algorithm for getting out of local minimum points. For this purpose, multiple-peak testing functions, which include Generalized Schwefel's Problem 2.26 (F2), Generalized Penalized Function 1 (F3), and Generalized Penalized Function 2 (F4), have been introduced by us.

In order to examine the role of different strategies in improving the mucilage algorithm, the test functions are used to perform optimality finding comparison experiments between the standard SMA, SMA with chaotic initialization only (BCSMA), SMA with dynamic nonlinear decreasing strategy only (DNSMA), SMA with fused sparrow warning mechanism and refractive reverse learning strategy only (SRSMA) and ISMA algorithms. For the precise appraisal of the strong points and weak points of the put-forward algorithms when they are compared with the benchmark algorithms, the population size is configured as 60, and the iteration number is set to 600. We put all the result outcomes in Table 1.

Table 1 gives the results of experiments which were done on five algorithms for some functions in dimensions of 20, 60, and 90. As the function dimension increases, the optimization difficulty rises and the solution accuracy decreases, but the ISMA algorithm presents better optimization performance in general. For the single-peak test function F1, the ISMA algorithm has the highest optimization accuracy at dimensions 20 and 60. Under the circumstance that the dimension is 90, the SRSMA algorithm can show bigger optimization accuracy and stability. This illustrates that the adding of Sobol sequence initiation and the Lévy flight pattern can effectively promote the convergence behavior of the algorithm in optimization process on various dimensions. As for the multi-peak test functions F2, F3, and F4, after we compare SMA, BCSMA, SRSMA, and DNSMA, the ISMA algorithm shows outstanding performance. This

hereby indicates that the promotion method which is put forward in this paper can effectively raise the optimization abilities of the algorithm. In the F4 test function, the ISMA algorithm's average optimization result is 3.33×100, this result is a obvious improvement when compared with the DNSMA model's comparatively good performance.

When we make comparison with the conventional SMA algorithm, the three single-strategy improved SMA algorithms have different degrees of improvement in the optimal value, mean and standard deviation, but the single-strategy improvement of SMA is limited, and the effect of optimization searching for different dimensions and test functions cannot be maintained. The ISMA algorithm fusing multiple strategies is better than the single strategy optimization algorithm in 20, 60 and 90 dimensional optimization in most of the optimization precision and stability, which verifies the all-round enhancement of the standard SMA algorithm by multi-strategy fusion.

Table 1: Optimization results of different improvement strategies

F	Model	D=20			D=60			D=90		
		Best	Mean	Std	Best	Mean	Std	Best	Mean	Std
F1	SMA	9.03×10^{-6}	3.43×10^{-5}	2.03×10^{-5}	3.25×10^{-1}	6.12×10^{-1}	2.34×10^{-1}	2.11×10^{1}	2.18×10^{1}	3.98×10^{0}
	ISMA	3.34×10^{-15}	1.52×10^{-13}	3.15×10^{-13}	2.67×10^{-4}	1.05×10^{-3}	7.56×10^{-4}	4.25×10^{-3}	2.65×10^{0}	2.05×10^{0}
	BCSMA	2.15×10^{-11}	2.23×10^{-10}	2.41×10^{-10}	7.66×10^{-4}	5.38×10^{-3}	4.02×10^{-3}	2.82×10^{0}	3.32×10^{0}	5.98×10^{-1}
	DNSMA	9.32×10^{-6}	3.25×10^{-5}	2.62×10^{-5}	3.85×10^{-1}	5.91×10^{-1}	1.76×10^{-1}	1.83×10^{1}	2.06×10^{1}	1.34×10^{0}
	SRSMA	5.01×10^{-1}	9.14×10^{-1}	2.62×10^{-1}	3.73×10^{0}	4.31×10^{0}	4.91×10^{-1}	1.45×10^{0}	1.71×10^{0}	5.72×10^{-1}
F2	SMA	-3.82×10^{3}	-3.51×10^{3}	2.54×10^{2}	-1.02×10^{4}	-9.63×10^{3}	4.81×10^{2}	-2.81×10^{4}	-2.63×10^{4}	1.07×10^{3}
	ISMA	-4.12×10^{3}	-3.82×10^{3}	2.41×10^{2}	-1.15×10^{4}	-1.01×10^{4}	6.85×10^{2}	-4.08×10^{4}	-3.77×10^{4}	5.15×10^{3}
	BCSMA	-3.84×10^{3}	-3.64×10^{3}	1.86×10^{2}	-1.04×10^{4}	-9.55×10^{3}	5.16×10^{2}	-2.65×10^{4}	-2.53×10^{4}	9.40×10^{2}
	DNSMA	-3.94×10^{3}	-3.84×10^{3}	1.38×10^{2}	-1.01×10^{4}	-9.34×10^{3}	4.17×10^{2}	-2.87×10^{4}	-2.62×10^{4}	1.11×10^{3}
	SRSMA	-3.62×10^{3}	-3.34×10^{3}	1.73×10^{2}	-9.82×10^{3}	-9.07×10^{3}	5.42×10^{2}	-3.93×10^{4}	-3.11×10^{4}	9.38×10^{2}
F3	SMA	6.27×10^{-8}	3.42×10^{-7}	2.22×10^{-7}	3.24×10^{-3}	7.55×10^{-3}	3.07×10^{-3}	3.25×10^{-1}	4.01×10^{-1}	4.06×10^{-2}
	ISMA	4.32×10^{-18}	6.62×10^{-16}	1.33×10^{-15}	5.08×10^{-4}	1.04×10^{-3}	5.17×10^{-4}	2.58×10^{-2}	1.42×10^{-1}	8.76×10^{-2}
	BCSMA	1.03×10^{-7}	4.52×10^{-7}	4.37×10^{-7}	5.71×10^{-3}	1.27×10^{-2}	5.31×10^{-3}	3.37×10^{-1}	4.22×10^{-1}	7.47×10^{-2}
	DNSMA	1.78×10^{-13}	2.53×10^{-12}	3.24×10^{-12}	2.98×10^{-4}	1.33×10^{-3}	1.27×10^{-3}	1.92×10^{-1}	2.56×10^{-1}	5.94×10^{-2}
	SRSMA	1.57×10^{-8}	1.17×10^{-2}	1.36×10^{-2}	1.77×10^{-1}	3.05×10^{-1}	1.12×10^{-1}	3.35×10^{-1}	3.75×10^{-1}	3.54×10^{-2}
F4	SMA	4.46×10^{-5}	1.76×10^{-4}	1.32×10^{-4}	2.58×10^{-3}	5.78×10^{-3}	3.62×10^{-3}	6.24×10^{0}	7.43×10^{0}	5.98×10^{-1}
	ISMA	1.92×10^{-8}	1.74×10^{-7}	2.31×10^{-7}	1.23×10^{-6}	2.22×10^{-3}	2.32×10^{-3}	3.31×10^{-1}	3.33×10^{0}	2.62×10^{0}
	BCSMA	5.12×10^{-5}	1.27×10^{-4}	6.26×10^{-5}	3.02×10^{-3}	6.52×10^{-3}	2.47×10^{-3}	5.35×10^{0}	7.46×10^{0}	9.84×10^{-1}
	DNSMA	4.63×10^{-8}	2.48×10^{-6}	3.12×10^{-6}	5.11×10^{-6}	1.11×10^{-3}	3.48×10^{-3}	1.12×10^{0}	3.81×10^{0}	1.93×10^{0}
	SRSMA	1.66×10^{-4}	1.58×10^{-1}	1.42×10^{-1}	1.68×10^{0}	2.33×10^{0}	2.76×10^{-1}	9.47×10^{-1}	7.32×10^{0}	2.32×10^{0}

To further validate the optimization performance of multi-strategy fusion improved mucilage algorithm for complex functions. Comparison experiments with the improved mucilage algorithms AOSMA, CESMA, and HSMAAOA are conducted for optimization searching on the selected CEC2017 test functions, respectively. They contain multi-peak (CEC05, CEC06), hybrid (CEC11, CEC16), and composite (CEC23, CEC24, CEC25) type functions.

The CEC2017 test functions with many local optimal solutions include mixed composite shift, rotate, and extended multimodal test functions that model the high complexity in the search domain. These combined test functions help to understand the ability to trade-off between exploitation and exploration by getting rid of local optima to eventually obtain a global optimal solution.

Setting the dimension as 60, the number of slime mold individuals as 60, and the number of iterations as 600, each algorithm performs 50 optimization searches for each test function separately, and the results are shown in Table 2. As can be seen from Table 2, the ISMA algorithm achieves better results in the optimization search for multi-peak, hybrid and composite functions. Compared with the other three improved mucilage algorithms, ISMA is more in line with the mucilage algorithm by proposing improvements from three aspects,

namely, population initialization, individual iteration and variant update.

Table 2: Optimization results of different improved SMA

F	SMA		ISMA		AOSMA		CESMA		HSMAAOA	
	Mean	Std	Mean	Std	Mean	Std	Mean	Std	Mean	Std
CEC05	6.06×10^{2}	3.02×10^{1}	5.82×10^{2}	2.51×10^{1}	6.06×10^{2}	4.11×10^{1}	5.88×10^{2}	2.62×10^{1}	5.95×10^{2}	3.65×10^{1}
CEC06	6.32×10^{2}	1.53×10^{1}	6.25×10^{2}	6.73×10^{0}	6.32×10^{2}	1.31×10^{1}	6.25×10^{2}	7.12×10^{0}	6.28×10^{2}	8.71×10^{0}
CEC11	1.25×10^{3}	7.15×10^{1}	1.22×10^{3}	3.32×10^{1}	5.91×10^{3}	9.68×10^{2}	1.27×10^{3}	3.82×10^{1}	1.27×10^{3}	6.58×10^{1}
CEC16	2.47×10^{3}	2.83×10^{2}	2.42×10^{3}	2.73×10^{2}	2.45×10^{3}	4.21×10^{2}	2.42×10^{3}	2.52×10^{2}	2.51×10^{3}	3.82×10^{2}
CEC23	2.77×10^{3}	1.88×10^{1}	2.74×10^{3}	1.73×10^{1}	3.48×10^{3}	7.58×10^{1}	2.74×10^{3}	2.54×10^{1}	2.74×10^{3}	2.48×10^{1}
CEC24	2.94×10^{3}	3.11×10^{1}	2.93×10^{3}	3.13×10^{1}	3.68×10^{3}	7.42×10^{1}	2.94×10^{3}	3.12×10^{1}	2.93×10^{3}	3.57×10^{1}
CEC25	2.91×10^{3}	1.97×10^{0}	2.88×10^{3}	1.37×10^{1}	2.91×10^{3}	4.46×10^{2}	2.91×10^{3}	1.42×10^{1}	2.87×10^{3}	9.63×10^{-1}

4 Case study and simulation verification

4.1 Analysis of case raw data

Example of wind and light power generation forecast data and day-ahead load forecast data through a local historical data prediction, the collection of local wind and photovoltaic power generation historical data, sampling interval of 2 min, to get the day-ahead wind and light load power prediction curves, wind and light load power difference, respectively, as shown in Fig. 3, Fig. 4, the purpose of the control algorithm, namely, to fill the power difference of the system with the optimal economy. One of the lithium storage system capacity of 60 kW/100 kW·h, hydrogen storage system 120 kW/200 kW·h.

Figure 5 shows the peak and valley tariff rules for a city's commercial electricity consumption, with a total of five electricity consumption peaks and peaks in the figure. The best arrangement method that is used in this research takes into consideration the difference that exists between peak and off-peak electric power prices. This target is to cut down or get rid of the charging work of the energy storage device inside the combined energy system in the time of high electricity prices. On the contrary, the load is mainly supplied by electric energy which is produced through wind power. At the same time, in the time periods when the electricity price is low, the energy storage system obtains electric energy from the power grid for the purpose of storage.

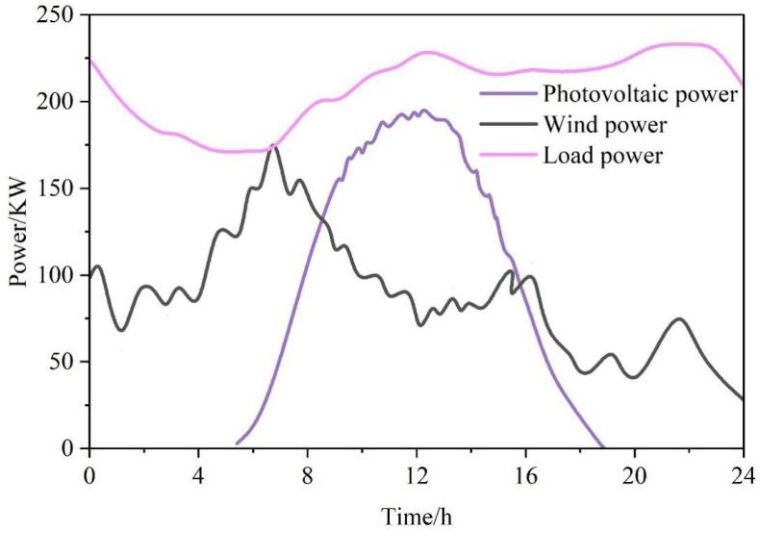

Figure 3: Day ahead forecasting curve of wind, photovoltaic and load power

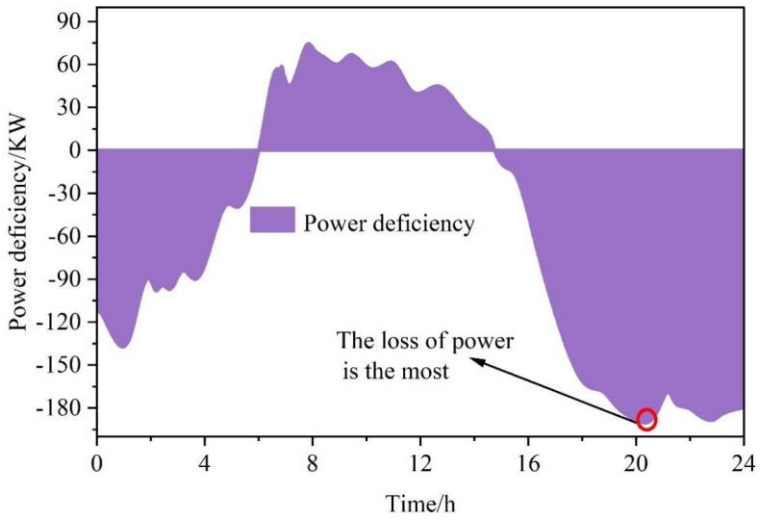

Figure 4: Power difference

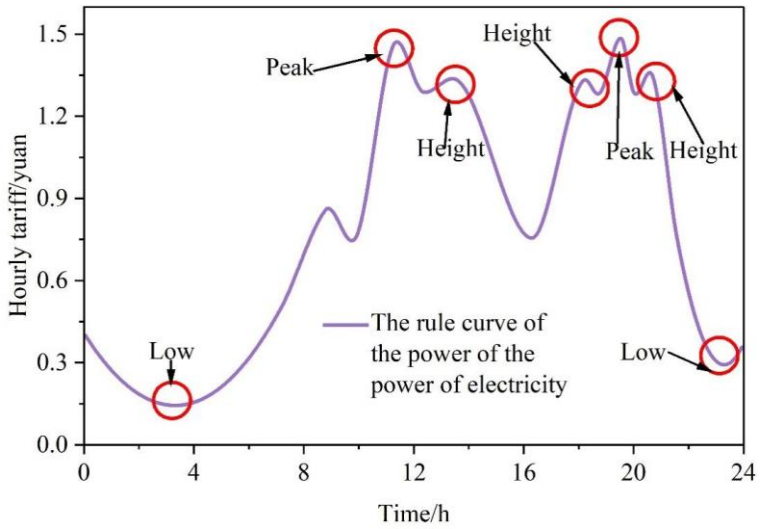

Figure 5: The rules of the price of the commercial power supply of a city

4.2 Optimized scheduling results

According to the above existing data combined with grid time-sharing tariffs brought into the summary of the day-ahead energy optimization scheduling strategy based on improved viscous bacteria algorithm for hydrogen energy utilization, the objective function is solved iteratively.The hydrogen system can make ascertainment of the lowest cost of the purchased electricity. Regarding the lithium energy-storage system, within the 24-hour scheduling that is arranged before the operation day, the optimized scheduling output of each kind of equipment which is inside the integrated energy system on the day before is displayed in Figure 6.

From Figure 6 combined with the time-sharing tariff curve can be seen, between 0:00 ~ 7:00, due to the wind power can not meet the load demand and the lower price of electricity, appropriate from the grid to purchase low-priced power resources to meet the load demand and charging or hydrogen energy storage; 7:00 ~ 17: 00 during the day, as the price of electricity to reach the peak, the load is increasing, this time the energy storage system output power sold power to assist the grid to balance the load During the daytime from 7:00 to 17:00, as the price of electricity reaches its peak and the load increases, the energy storage system sells power to assist the grid in balancing the load and obtaining a large economic return; at night from 17:00

to 24:00, the energy storage system again buys low-priced power for energy storage in preparation for the next day of operation. Through the optimized scheduling of hydrogen and lithium energy storage systems, the wind and light utilization rate can be maximized, wind and light abandonment can be reduced and the grid scheduling pressure can be alleviated, in addition, the energy storage operator can also obtain a large economic return.

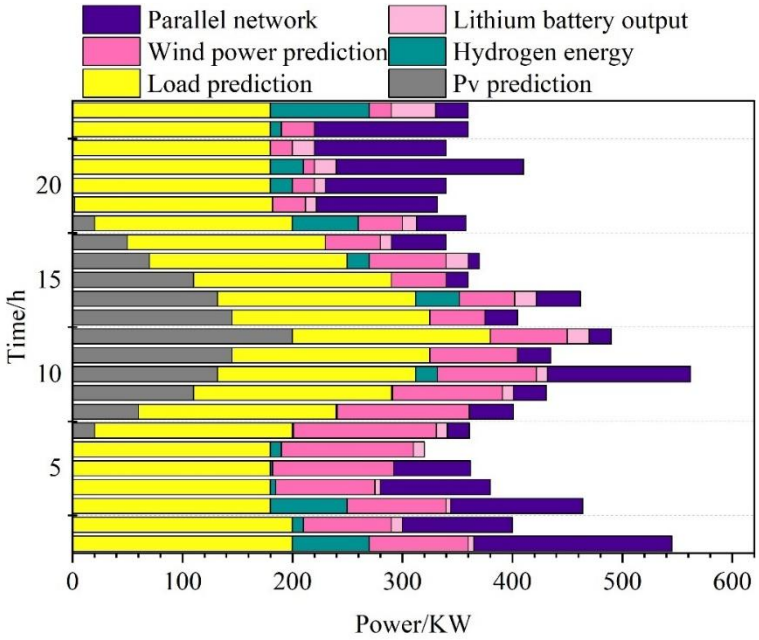

Figure 6: All kinds of equipment has been optimized for scheduling

The optimized output curves and the change curves of charge state/hydrogen pressure state of lithium storage and hydrogen storage systems a few days ago are shown in Figs. 7 and 8. According to what is shown in Figures 7 and 8, the hydrogen storage system reflects the condition of a lithium storage electricity cut-off. To speak specifically, it carries out charging (hydrogen making) for energy storing between 0:00 and 7:00. This circumstance happens on condition that the cost of grid electricity is low, or when the wind and photovoltaic power generation quantity is at a relatively high level. On the opposite side, it outputs electric energy (it uses hydrogen fuel cell to carry out power generation) when the price of grid electric power is at a high level and the wind and photovoltaic power generation are not enough to satisfy the demand of the load. After the wind-photovoltaic-hydrogen-storage combined energy system obtains the superior day-ahead scheduling instructions, the day-ahead optimization scheduling method put forward in this paper uses the wind-photovoltaic load forecast data and one city's peak-valley electricity price data. This strategy’s target is to carry out optimization on the output of next day of the integrated energy system’s hydrogen storage system and lithium battery storage system. In this procedure, the number of hydrogen manufacture and the quantum of hydrogen fuel cell electricity generation are utilized to indicate the charge and discharge behaviors of the hydrogen storage system. Through the careful arrangement of hydrogen output production, fuel cell electric power, and the charge and discharge power of the lithium battery energy storage system, the wind-photovoltaic-hydrogen-storage combined energy system can effectively track the electric power generation plan. Furthermore, it can make guarantee that the system obtains the most big economic benefits through the electricity trading of it.

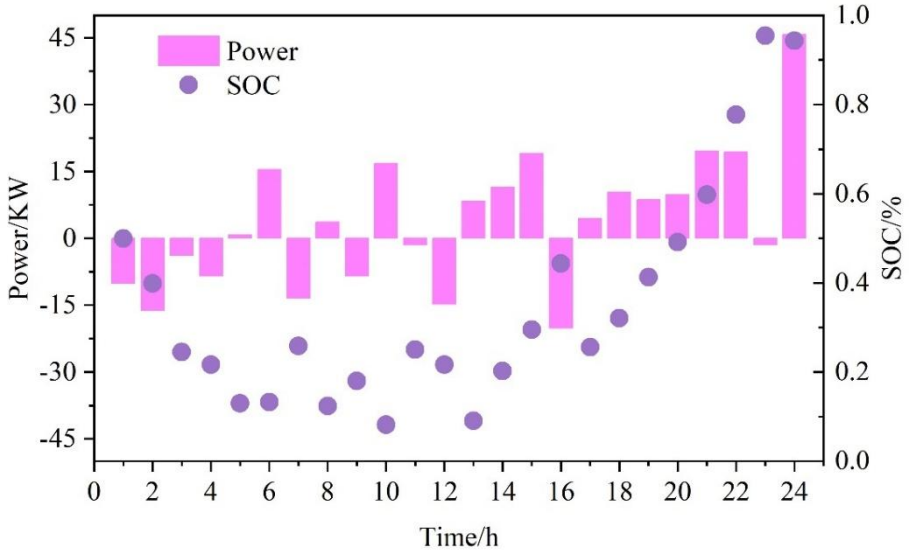

Figure 7: The lithium energy storage is optimized and SOHP

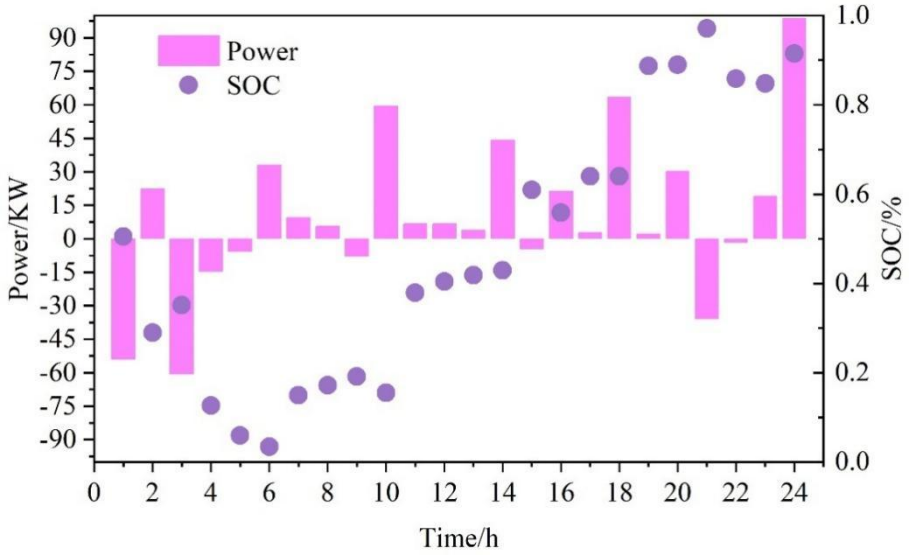

Figure 8: The hydrogen storage system has been optimized and SOHP

4.3 Analysis of program economics and profit sharing

4.3.1 Results of programmatic economic analysis

Table 3 shows the economic indicators of P2G equipment under different investment modes. The net profit of P2G equipment in Scenarios 2 and 3 is negative, because the depreciation cost of P2G equipment is high, and it is difficult to ensure sufficient operating hours of P2G equipment only by relying on wind and light abandonment, and the lower utilization rate of P2G equipment results in a loss situation. The P2G equipment in Scenario 4 and Scenario 5 are able to realize 24h full load operation, and the revenue of P2G equipment is the same under the two scenarios, however, the complementary operation of wind-light-fire in Scenario 5 makes the operation cost of P2G equipment lower, and the net revenue of P2G equipment in Scenario 5 is 54,712 RMB higher than that of Scenario 4. To sum up, the cooperative operation among wind energy enterprises, photovoltaic energy enterprises and thermal power enterprises can ensure the optimal economic benefit of P2G equipment, and therefore can achieve the

maximum possible income.

Table 3: The four types of investment cases are economical

Project	Solution 2	Solution 3	Solution 4	Solution 5
Equipment gains/yuan	67239	38445	823659	823415
Equipment running cost/yuan	28754	16543	327189	273125
Equipment depreciation/yuan	115069	115079	115077	115089
Net profit/yuan	-76658	-93185	381469	436181

4.3.2 Results of profit-sharing analysis

The results of benefit distribution through the traditional Shapley value method are shown in Table 4.The profit distribution based on equal distribution does not take into account the investment ratio of each subject, the profit distribution obtained by the wind power enterprise is 37568.1 yuan, but the depreciation cost of its investment is 51,133.5 yuan, at this time, the wind power enterprise will be in a loss position when it invests in P2G equipment, which will be unfavorable to the stability of the whole joint venture alliance. Based on the classic Shapley value method for profit redistribution, the wind power enterprise obtains the profit distribution of 65214.8 yuan, the photovoltaic enterprise obtains the profit distribution of 25481.8 yuan, and the thermal power enterprise obtains the profit distribution of 460578.5, at this time, the total profit distribution of the operation of the P2G equipment is more balanced, and it can make all the parties involved to obtain the benefits. Therefore, the traditional Shapley value method can take into account each entity's initial investment proportion, and make the income distribution become more equitable and reasonable.

Table 4: Distribution of profits based on improved shapley method

Project	Wind power enterprise	Photovoltaic enterprise	Coal-fired power corporation
Distribution of profits based on equal distribution /yuan	37568.1	19555.1	494245.3
Equity ratio/%	57.14	14.29	28.57
Investment day depreciation amount/yuan	51133.5	12789.1	25571.3
Shapley method profit allocation/yuan	65214.8	25481.8	460578.5
Daily operating profit/yuan	923015	215044	8334
Total income/yuan	937085.5	227835.2	443322.6

5 Conclusion

This research thesis focuses on the demands for economic and continuable development inside the new-energy hydrogen production project, constructs a new energy hydrogen production operation mode with multi-principal joint venture, designs a day-ahead optimized output scheduling of wind-optical-hydrogen-storage integrated energy system based on the improved viscous bacterial algorithm, and finally obtains an energy storage output scheme with the highest economic efficiency of electricity trading for the wind-optical-hydrogen-storage integrated energy system.

The result of the simulation experiments on the benchmark test function and the CEC2017 test function show that ISMA, which integrates Sobol sequence initialization and Lévy flight,

has better collaborative complementarity, and the test results under 20, 60 and 90 dimensions have better optimization result enhancement compared to the standard SMA, and compared to the other improved viscous bacterial algorithms AOSMA, CESMA, HSMAAOA can achieve better optimization results than other improved mucilage algorithms AOSMA, CESMA, HSMAAOA.

The cooperative optimization scheduling strategy based on the improved slime mold algorithm makes full use of the mechanism of time-sharing tariff, charging or hydrogen storage when the tariff is low. During the daytime when the electricity price reaches the peak, the energy storage system contributes to assist the grid to balance the load demand. At night, the energy storage system continues to purchase low-priced electricity to complete the energy storage, in order to maximize the utilization rate of wind and light, and obtain more economic benefits.

The operation mode of new-energy hydrogen making which includes multiple bodies effectively combines the output characteristics of different power supplies. It overcomes the price difficulties that exist in the investment and operation model that uses one single body. Under the premise that comprehensive operating costs are lower, the production capacity of P2G equipment is fully utilized by it. Furthermore, the pure profit in Scenario 5 is 54,712 yuan more than the one in Scenario 4. The profit distribution scheme based on the classical Shapley value method can reasonably distribute the benefits due to each subject according to the corresponding ratio based on the subject's participation and contribution, which maximizes the benefits of all parties and ensures that the results are fair and reasonable while mobilizing the enthusiasm of each subject's participation.

About the Author

Shilong Liu (born June 1984), male, ID number: 610404198406042516, Han ethnicity, native of Xianyang, Shaanxi Province, holds a bachelor's degree and is a senior engineer specializing in water conservancy and hydropower engineering, as well as new energy project construction management.

Chengbang Ma (born October 1985, ID: 10040033), male, Han ethnicity, from Ledu, Qinghai Province, holds a bachelor's degree and works as an engineer specializing in new energy project construction management, as well as operation, maintenance, and management of new energy power stations.

References

[1] Lin, B., & Li, Z. (2022). Towards world's low carbon development: The role of clean energy. Applied Energy, 307, 118160.

[2] Li, C., Shah, N., Li, Z., & Liu, P. (2024). Modelling of wind and solar power output uncertainty in power systems based on historical data: A characterisation through deterministic parameters. Journal of Cleaner Production, 484, 144233.

[3] Ren, G., Liu, J., Wan, J., Wang, W., Fang, F., Hong, F., & Yu, D. (2021). Investigating the complementarity characteristics of wind and solar power for load matching based on the typical load demand in China. IEEE Transactions on Sustainable Energy, 13(2), 778-790.

[4] Burke, P. J., Widnyana, J., Anjum, Z., Aisbett, E., Resosudarmo, B., & Baldwin, K. G. (2019). Overcoming barriers to solar and wind energy adoption in two Asian giants: India and Indonesia. Energy Policy, 132, 1216-1228.

[5] Zhang, J., & Huang, W. (2022). A pilot assessment of new energy usage behaviors: The impacts of environmental accident, cognitions, and new energy policies. Frontiers in Environmental Science, 10, 955999.

[6] Welder, L., Stenzel, P., Ebersbach, N., Markewitz, P., Robinius, M., Emonts, B., & Stolten, D. (2019). Design and evaluation of hydrogen electricity reconversion pathways in national energy systems using spatially and temporally resolved energy system optimization. International Journal of Hydrogen Energy, 44(19), 9594-9607.

[7] Glenk, G., & Reichelstein, S. (2019). Economics of converting renewable power to hydrogen. Nature Energy, 4(3), 216-222.

[8] Hofrichter, A., Rank, D., Heberl, M., & Sterner, M. (2023). Determination of the optimal power ratio between electrolysis and renewable energy to investigate the effects on the hydrogen production costs. International Journal of Hydrogen Energy, 48(5), 1651-1663.

[9] Gutiérrez-Martín, F., Amodio, L., & Pagano, M. (2021). Hydrogen production by water electrolysis and off-grid solar PV. International Journal of Hydrogen Energy, 46(57), 29038-29048.

[10] Shin, H., Jang, D., Lee, S., Cho, H. S., Kim, K. H., & Kang, S. (2023). Techno-economic evaluation of green hydrogen production with low-temperature water electrolysis technologies directly coupled with renewable power sources. Energy Conversion and Management, 286, 117083.

[11] Egeland-Eriksen, T., Jensen, J. F., Ulleberg, Ø., & Sartori, S. (2023). Simulating offshore hydrogen production via PEM electrolysis using real power production data from a 2.3 MW floating offshore wind turbine. international journal of hydrogen energy, 48(74), 28712-28732.

[12] Horri, B. A., & Ozcan, H. (2024). Green hydrogen production by water electrolysis: Current status and challenges. Current opinion in green and sustainable chemistry, 47, 100932.

[13] Radner, F., Strobl, N., Köberl, M., Winkler, F., Esser, K., & Trattner, A. (2024). Off-grid hydrogen production: Analysing hydrogen production and supply costs considering country-specifics and transport to Europe. International Journal of Hydrogen Energy, 80, 1197-1209.

[14] Chowdhury, P., Islam, T., & Agyekum, E. B. (2025). Techno-economic and multicriteria analysis of grid-connected energy systems for hydrogen production: a case study from Bangladesh. International Journal of Hydrogen Energy, 109, 95-114.

[15] Fan, G., Liu, Z., Liu, X., Shi, Y., Wu, D., Guo, J., ... & Zhang, Y. (2022). Two-layer collaborative optimization for a renewable energy system combining electricity storage, hydrogen storage, and heat storage. Energy, 259, 125047.

[16] Wei, F., Sui, Q., Li, X., Lin, X., & Li, Z. (2021). Optimal dispatching of power grid integrating wind-hydrogen systems. International Journal of Electrical Power & Energy Systems, 125, 106489.

[17] Niu, M., Li, X., Sun, C., Xiu, X., Wang, Y., Hu, M., & Dong, H. (2023). Operation optimization of wind/battery storage/alkaline electrolyzer system considering dynamic hydrogen production efficiency. Energies, 16(17), 6132.

[18] Farag, H. E., Al-Obaidi, A., Khani, H., El-Taweel, N., El-Saadany, E. F., & Zeineldin, H. H. (2020). Optimal operation management of distributed and centralized electrolysis-based hydrogen generation and storage systems. Electric Power Systems Research, 187, 106476.

[19] Guo, H., Zhang, C., Wang, J., Wu, Z., Wang, T., Wang, P., ... & Yu, F. (2025). Design and operation schedule of RES hydrogen production system with downstream constraints. International Journal of Hydrogen Energy, 102, 68-79.

[20] Liu, X. (2022). Optimal scheduling strategy of electricity-heat-hydrogen integrated energy system under different operating modes. International journal of energy research, 46(9), 12901-12925.

[21] Sun, J., Peng, Y., Lu, D., Chen, X., Xu, W., Weng, L., & Wu, J. (2022). Optimized configuration and operating plan for hydrogen refueling station with on-site electrolytic production. Energies, 15(7), 2348.

[22] Wu, X., Li, H., Wang, X., & Zhao, W. (2020). Cooperative operation for wind turbines and hydrogen fueling stations with on-site hydrogen production. IEEE Transactions on Sustainable Energy, 11(4), 2775-2789.